Electronic Supplementary Material (ESI) for RSC Advances.

Supporting Information

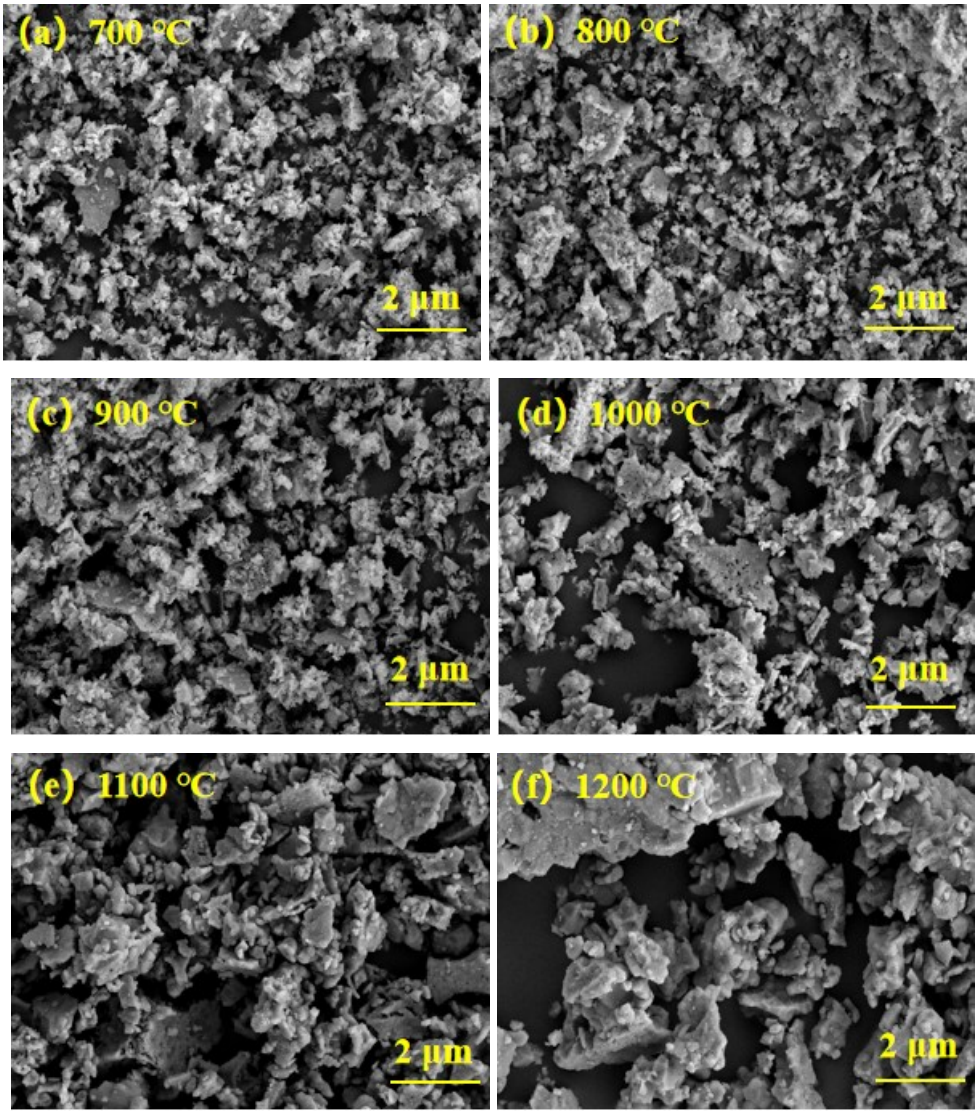

Fig S1 (a) - (f) SEM of the STFN samples at different calcination temperatures

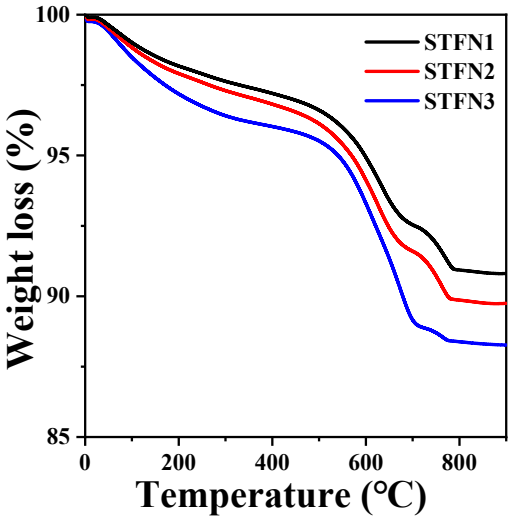

Fig S2 TGA of S_{1-x}TFN with an A-site vacancy

Table S1 Comparison of pore size and specific surface area of STFN at different calcination temperatures

Catalysts	Surface area (m^2/g)	Pore volume (cm^3/g)	Pore width (nm)
STFN-700	32.839	0.104	3.828
STFN-800	33.933	0.050	3.939
STFN-900	25.549	0.047	3.806
STFN-1000	17.106	0.021	3.677
STFN-1100	8.404	0.012	3.539
STFN-1200	6.001	0.007	3.420

Table S2 ORR performance of sample STFN at different calcination temperatures

Catalysts	E_{onset} (V vs. RHE)	$E_{1/2}$ (V vs. RHE)	J ($mA\ cm^{-2}$)	Tafel ($mV\ dec^{-1}$)
STFN-700	0.8843	0.6151	-5.8040	106
STFN-800	0.8857	0.6411	-6.1971	103
STFN-900	0.8821	0.5961	-5.5891	123
STFN-1000	0.8812	0.5678	-5.3766	126
STFN-1100	0.8793	0.5318	-5.1958	129
STFN-1200	0.8762	0.5221	-4.0324	140

Table S3 OER performance and ΔE of STFN calcined at different temperatures

Catalysts	OER			ORR	ΔE (V)
	Tafel ($mV\ dec^{-1}$)	η (mV)	@10 $mA\ cm^{-2}$ (V)	@-3 $mA\ cm^{-2}$ (V)	
STFN-700	127	450.6	1.6806	0.6001	1.0805
STFN-800	103	412.0	1.6420	0.6124	1.0296
STFN-900	136	463.3	1.6933	0.5972	1.0961
STFN-1000	153	526.3	1.7563	0.5815	1.1748
STFN-1100	159	553.3	1.7833	0.5279	1.2554

STFN-1200	211	568.3	1.7983	0.5128	1.2855

Table S4 A-site-deficient STFN pore size and specific surface area data comparison

Catalysts	Surface area (m^2/g)	Pore volume (cm^3/g)	Pore width (nm)
STFN1	32.839	0.104	3.828
STFN2	34.957	0.112	3.941
STFN3	36.828	0.153	4.154

Table S5 Oxygen species content of STFN1 and STFN3

Catalyst	H_2O (%)	-OH/O_2 (%)	O_2^{2-}/O^- (%)	O_{latt} (%)
STFN1	11.28	32.34	35.37	21.01
STFN3	1.49	41.96	42.91	13.64

Table S6 Fe and Ni contents in STFN1 and STFN3

Catalyst	Fe^{4+} (%)	Fe^{3+} (%)	Ni^{3+} (%)	Ni^{2+} (%)
STFN1	30.37	69.63	60.96	39.04
STFN3	40.08	59.92	64.42	35.58

Table S7 ORR performance of A-site-deficient STFN samples

Catalysts	E_{onset} (V)	$E_{1/2}$ (V)	J (mA cm^{-2})	Tafel (mV dec^{-1})
STFN1	0.8857	0.6411	-6.1971	103
STFN2	0.8912	0.6679	-6.5671	98
STFN3	0.8934	0.6740	-6.9762	97

Table S8 OER performance and ΔE of A-site-deficient STFN samples

Catalysts	OER			ORR	ΔE（V）
	Tafel（mV dec^{-1}）	η（mV）	@10 mA cm^{-2}（V）	@-3 mA cm^{-2}（V）	
STFN1	103	412.0	1.6420	0.6124	1.0296
STFN2	100	408	1.6380	0.6345	1.0335
STFN3	99	399.9	1.6299	0.7082	0.9217

Table S9 A comparison of ORR and OER activity for STFN3 and other reported perovskite catalysts. All the electrochemical measurements were carried out in 0.1 M KOH solution

Catalyst	ORR		OER			Ref.
	$E_{1/2}$ (V vs. RHE)	Tafel (mV dec^{-1})	Tafel (mV dec^{-1})	η (mV) @10 mA cm^{-2}	ΔE (V)	
$(La_{0.8}Sr_{0.2})_{0.95}Mn_{0.5}Fe_{0.5}O_{3-\delta}$	-0.124	132	230	-	-	[1]
$Ba_{0.5}Sr_{0.5}Co_{0.8}Fe_{0.2}O_{3-\delta}$	-	-	-	380	-	[2]
$Ba_{0.5}Sr_{0.5}Co_{0.8}Fe_{0.2}O_{3-\delta}$	-	-	94	510	-	[3]
$La_{0.8}Sr_{0.2}Co_{0.4}Mn_{0.6}O_{3-\delta}$	0.888	90	113	506	1.032	[4]
$La_{0.8}Sr_{0.2}Co_{0.6}Mn_{0.4}O_{3-\delta}$	0.881	104	113	515	1.104	[4]
$Sr_{0.95}Nb_{0.1}Co_{0.7}Fe_{0.2}O_{3-\delta}$	-	-	70	420	-	[5]
$La_{0.7}Sr_{0.15}Pd_{0.15}MnO_{3-\delta}$	0.973	87	-	-	-	[6]
$La_{0.9}Y_{0.1}MnO_{3-\delta}$	0.909	101	-	-	-	[7]
$La_{1.7}Sr_{0.3}Co_{0.5}Ni_{0.5}O_{4+\delta}$	0.696	-	125	592	1.126	[8]
$La_{0.4}Sr_{0.6}Co_{0.7}Fe_{0.2}Nb_{0.1}O_{3-\delta}$	0.505	114	78	360	1.07	[9]
$BaZr_{0.15}Fe_{0.85}O_{3-\delta}$	-	-	97	471	-	[10]
IrO_2	-	-	115	413	-	This work
Pt/C	0.7054	99	-	-	-	This work
$Sr_{0.9}Ti_{0.3}Fe_{0.6}Ni_{0.1}O_{3-\delta}$	0.7082	97	99	399.9	0.9217	This work

References

[1] R-H Yuan, Y He, W He, et al. Bifunctional electrocatalytic activity of $La_{0.8}Sr_{0.2}MnO_3$-based perovskite with the A-site deficiency for oxygen reduction and evolution reactions in alkaline media[J]. Applied Energy, 2019, 251:113406.

[2] G Li, S Hou, L Gui, et al. Carbon quantum dots decorated $Ba_{0.5}Sr_{0.5}Co_{0.8}Fe_{0.2}O_{3-\delta}$ perovskite nanofibers for boosting oxygen evolution reaction[J]. Applied Catalysis B: Environmental, 2019, 257:117919.

[3] Y Bu, O Gwon, G Nam, et al. A Highly Efficient and Robust Cation Ordered Perovskite Oxide as a Bifunctional Catalyst for Rechargeable Zinc-Air Batteries[J]. ACS Nano, 2017, 11(11): 11594-11601.

[4] Q Wang, Y Xue, S Sun, et al. $La_{0.8}Sr_{0.2}Co_{1-x}MnxO_3$ perovskites as efficient bi-functional cathode catalysts for rechargeable zinc-air batteries[J]. Electrochimica Acta, 2017, 254: 14-24.

[5] H Liu, X Ding, L Wang, et al. Cation deficiency design: A simple and efficient strategy for promoting oxygen evolution reaction activity of perovskite electrocatalyst[J]. Electrochimica Acta, 2018, 259: 1004-1010.

[6] Y Xue, S Sun, Q Wang, et al. $La_{0.7}(Sr_{0.3-x}Pd_x)MnO_3$ as a highly efficient electrocatalyst for oxygen reduction reaction in aluminum air battery[J]. Electrochimica Acta, 2017, 230: 418-427.

[7] H Miao, Z Wang, Q Wang, et al. A new family of Mn-based perovskite ($La_{1-x}Y_xMnO_3$) with improved oxygen electrocatalytic activity for metal-air batteries[J]. Energy, 2018, 154: 561-570.

[8] P Li, B Wei, Z Lü, et al. $La_{1.7}Sr_{0.3}Co_{0.5}Ni_{0.5}O_{4+\delta}$ layered perovskite as an efficient bifunctional electrocatalyst for rechargeable zinc-air batteries[J]. Applied Surface Science, 2019, 464: 494-501.

[9] L Yu, N Xu, T Zhu, et al. $La_{0.4}Sr_{0.6}Co_{0.7}Fe_{0.2}Nb_{0.1}O_{3-\delta}$ perovskite prepared by the sol-gel method with superior performance as a bifunctional oxygen electrocatalyst[J]. International Journal of Hydrogen Energy, 2020, 45(55): 30583-30591.

[10] K Zhu, H Liu, X Li, et al. Oxygen evolution reaction over Fe site of $BaZr_xFe_{1-x}O_{3-\delta}$ perovskite oxides, Electrochim. Acta, 241 (2017) 433-439.